Chapter 6: Steam reactivity experiments

6.1. Introduction

In this chapter, all aspects regarding the reactivity experiments are discussed. Section 6.2 provides a detailed discussion of the chemicals used during experimentation, the experimental equipment and specifications, as well as the procedure followed to conduct the experiments. The experimental results obtained from the steam gasification experiments, using the 5 mm and 10 mm particles, are presented in Section 6.3, and Section 6.4 concludes this chapter with a summary.

6.2. Experimental methodology

6.2.1. Chemicals

The chemicals used for the reactivity experiments include: coal particles (raw particles, as well as catalyst-bearing particles), deionised water and nitrogen (N_2) gas. The coal used for this study was supplied by SGS laboratories, as discussed in Section 4.2. The coal characterisation results are presented in Section 4.5.

Deionised water, which was also used for the impregnation solutions, was used for the steam gasification experiments. The N_2 gas used for the experiments was supplied by African Oxygen Limited (Afrox), and is of ultra high purity grade (UHP), with a purity of >99.999%.

6.2.2. Experimental set-up

The TGA (Thermogravimetric analyser) used for the steam gasification experiments was constructed in-house, and was designed specifically for reactivity experimentation with large coal particles (up to 40 mm). During experimentation, the temperature of the furnace and the weight of the sample are measured as a function of time, and the experimental data is logged on a computer. Figure 6.1 is a schematic representation of the laboratory setup of the large particle TGA.

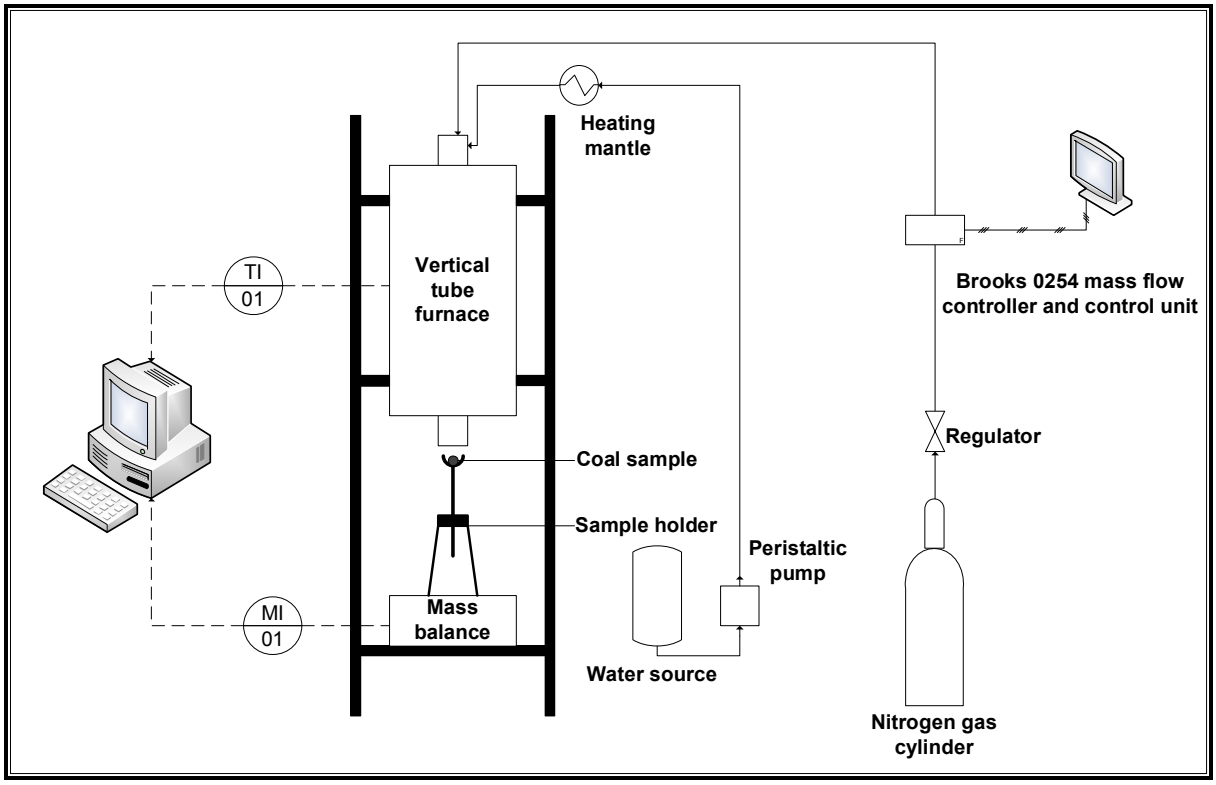

Figure 6.1: Experimental set-up of the large particle TGA

The Elite Thermal Systems Ltd. furnace, as pictured above, is a model TSV 15/50/180 vertical tube furnace and was supplied by Lenton. The furnace can reach a maximum temperature of 1500 °C, with variable heating rates. The vertical tube furnace is equipped with a K-type thermocouple, which measures the temperature of the reaction zone. This furnace is also fitted with a Eurotherm 2216 temperature controller and a Eurotherm 2416 microprocessor programmable controller, which controls the furnace temperature at the set point temperature.

The TGA is equipped with a steam generation unit, which consists of a stainless steel container, a peristaltic pump and a heating mantle. The stainless steel container is filled with deionised water during experimentation, and has a storage capacity of 10 L. Water is pumped from the container to the furnace with a 323 S/D Watson-Marlow Bredel high-performance variable speed pump. The steam is generated by pumping the water through a heating mantle before it enters the furnace. This heating mantle has a maximum temperature of 400 °C, and the temperature is measured with a K-type thermocouple. N_2 gas is fed to the furnace through a plastic tube, and the gas flow rate is controlled with a Brooks model 0254 mass flow controller. The steam, as well as the N_2 gas, is introduced at the top of the furnace.

The sample weight is continually measured during experimentation with a Radwag precision PS 750/C/2 balance. The coal sample is placed in a specially designed sample holder, consisting of a stainless steel tripod stand and a conically shaped quartz bucket and rod, which is placed on the mass balance.

The specifications of the main components of the large particle TGA are presented in Table 6.1.

Table 6.1: Equipment specifications for large particle TGA

	Specification
Furnace	**Model TSV 15/50/180**
Temperature range	Ambient -1500 °C
Heating rates	1-20 °C/min
Reaction zone diameter	50 mm
Sample size	5-40 mm
Sample weight	± 200 g
Pump	**Model 323 S/D**
Speed range	0.3-400 rpm
Maximum flow rate	2 L/min
Mass balance	**Model PS 750/C/2**
Maximum capacity	750 g
Accuracy	1 mg

6.2.3. Experimental procedure and specifications

Raw and impregnated coal samples were used for the steam reactivity experiments, and particles were selected as described in Section 5.3.1.

Isothermal gasification experiments were performed, which implies that the entire reaction occurs at a constant operating temperature. The furnace was set to a specified experimental temperature, with a heating rate of 20 °C/min, and the N_2 gas was simultaneously introduced to the furnace. Once the furnace had stabilised at the specified temperature, the sample holder was placed on the mass balance and the furnace was lowered over the holder. The mass balance was tared to zero under these conditions in order to eliminate weight fluctuations due to gas flow. Once the mass balance had been

tared, the furnace was raised to remove the sample holder and the selected coal sample was loaded into the quartz bucket. A sufficient amount of coal sample for a particular size range was selected in order to obtain a sample representative of the bulk coal sample. This amounted to the utilisation of samples with a mass of approximately 3-6 g (up to 20 particles), depending on the particle size. Once the sample had been loaded into the bucket, the sample holder was again placed on the mass balance. The data acquisition programme was initialised before the furnace was lowered over the coal sample. The sample mass was monitored to determine when devolatilisation of the coal sample was complete. After devolatilisation was completed, the coal sample was kept under inert conditions for 10 minutes, at operating temperature, to ensure isothermal particle temperature. After the additional waiting period, the pump was turned on and the steam was introduced to the furnace. The gasification of the coal sample was allowed to progress until no further mass loss was observed. The experimental temperature, as measured just above the coal sample, was continuously measured throughout the gasification experiments (A temperature profile is given in Appendix B.6), and no significant temperature change due to reaction could be observed. Upon completion of the gasification reaction, the pump and the furnace were switched off, while the ash sample was allowed to cool in the furnace in an inert atmosphere. Once the ash sample had cooled down, the furnace was raised and the sample was removed from the bucket.

The experimental data of interrupted runs were still used in cases where runs were interrupted due to external factors such as power failures. The coal sample was left in the oven and allowed to combust in air, in order to obtain the final mass of the ash sample. This value was used to construct conversion-time graphs from the mass loss data.

The operating conditions/specifications used to evaluate the steam gasification experiments are summarised in Table 6.2:

Table 6.2: Reaction specifications for gasification experiments

Variable	Specification
Coal sample	Medium rank-C bituminous Highveld coal (raw and impregnated)
Reagents	N_2 gas, steam
Operating temperature	800 °C, 825 °C, 850 °C, 875 °C
Temperature profile	Isothermal
Operating pressure	Ambient pressure (≈ 87.5 kPa)

Steam concentration	80 mol%
Coal particle size	5 mm, 10 mm

6.3. Results and discussion

The experimental results obtained from the steam gasification experiments are presented in this section, and the discussion of experimental results will focus on normalisation of experimental data, factors influencing reactivity, kinetic evaluation and the structural changes observed during experimentation.

6.3.1. Normalisation of experimental results

A data acquisition programme is used to attain experimental data, and the unprocessed experimental data are given as sample mass loss as a function of time. The experimental mass loss data, as well as the normalised mass loss data, for the raw 5 mm particles at 825 ℃ are given in Figure 6.2 and Figure 6.3, respectively. The data acquired during experimentation is sampled to between 250 and 300 data points to obtain the normalised mass loss curve. (All experimental results obtained for uncatalysed coal are termed “raw”, while results obtained for the impregnated coal are termed “cat”).

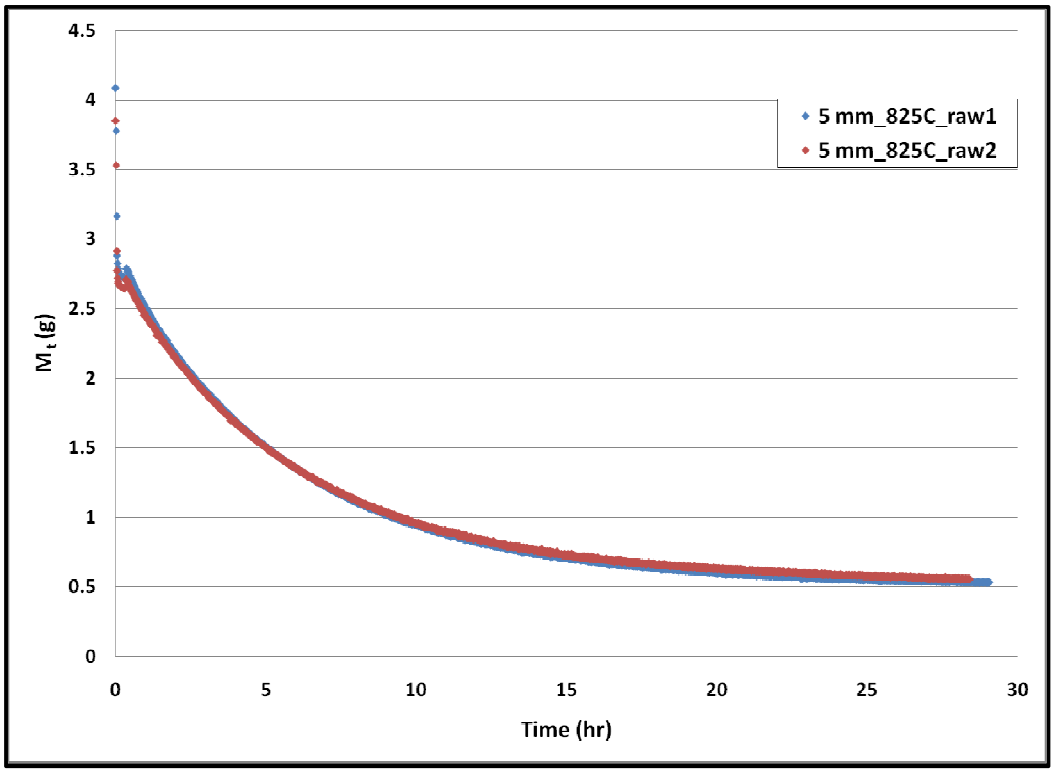

Figure 6.2: Mass loss curve for raw 5 mm particles, at 825 ℃

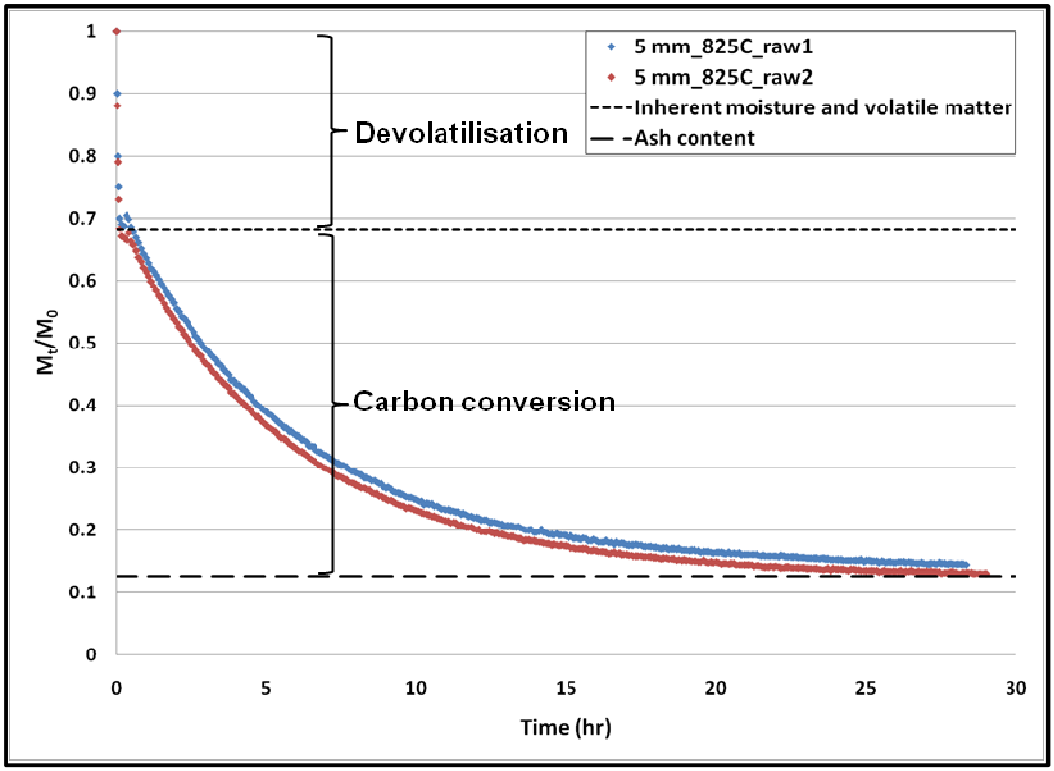

Figure 6.3: Normalised mass loss curve for raw 5 mm particles, at 825 °C

As seen from Figure 6.3, the mass loss data can be divided into two phases, devolatilisation and carbon conversion. The initial mass loss phase, or devolatilisation, is due to the release of inherent moisture and volatile matter and occurs in an inert atmosphere. The period of devolatilisation is approximately 6 minutes for all experiments (5 mm and 10 mm). During the second mass loss phase, carbon conversion occurs due to the introduction of steam to the system. Conversion-time graphs can be constructed from the mass loss data by using the following equation:

$$X = \frac{M_0 - M_t}{M_0 - M_{ash}} \qquad \text{(Equation 6.1)}$$

where X is the carbon conversion, M_0 is the initial sample weight at the start of gasification, M_t is the sample weight at any given time t, and M_{ash} is the weight of the remaining ash after the reaction is complete. The conversion-time graphs are obtained by only considering the mass loss which occurs during carbon conversion. The final sample weight, which is the mass of the residual ash, is compared with the ash content as determined by the proximate analysis. It was found that the final experimental ash values had a deviation of ± 4 %, when compared to the proximate analysis value. The experimental inherent moisture and volatile matter values, as well as the ash values, are presented in Appendix B.

The following conversion graph is obtained from the normalised mass loss data in Figure 6.3:

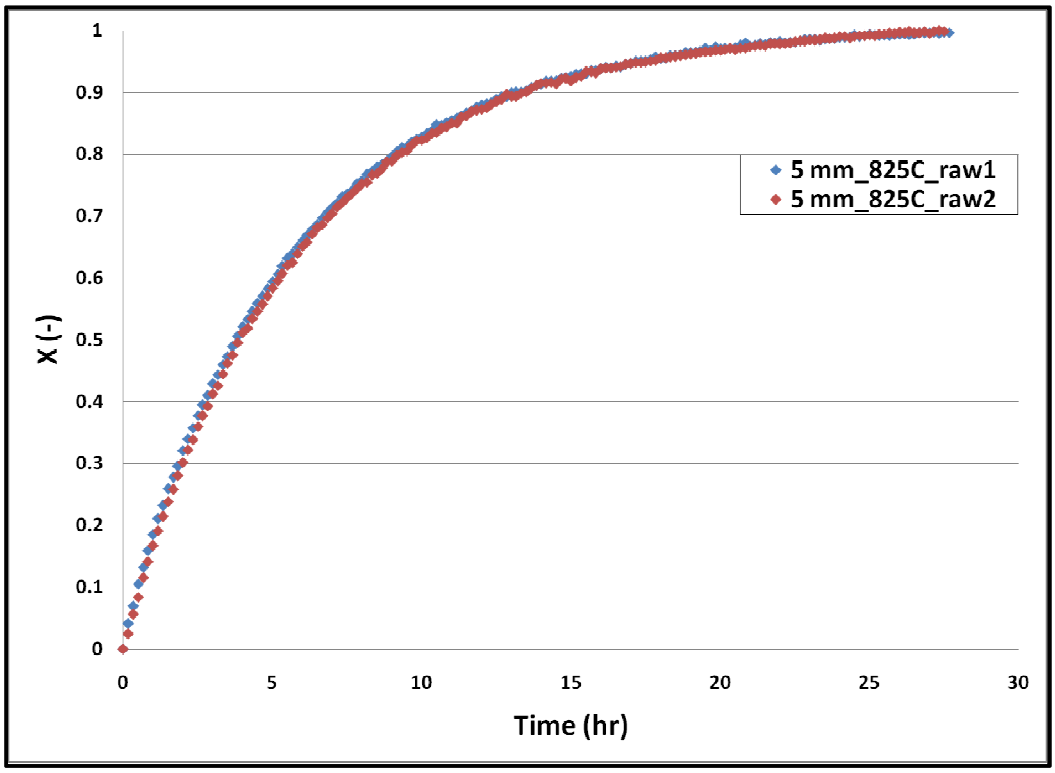

Figure 6.4: Conversion-time graph for raw 5 mm particles, at 825 ℃

The normalised mass loss data is sampled to between 100 and 150 data points to obtain the conversion-time graphs, as pictured in Figure 6.4. All steam gasification reactions were performed in duplicate, and an average error between duplicate runs was determined in order to validate the reproducibility of the experimental data. Conversion-time graphs for all duplicate experiments are presented in Appendix B, along with the average errors obtained for the experimental data.

The experimental data from the duplicate runs were used to obtain an average for each set of experiments conducted, and were further sampled to between 30 and 40 data points. The results presented in the subsequent sections of this chapter are the average data obtained from the experimental runs.

6.3.2. Influence of impregnation

The effect of impregnation was investigated in order to determine whether the increase in reaction rate was in fact due to the catalytic effect, or rather due to the change in particle

structure. This was done by submerging 5 mm and 10 mm particles in deionised water, for the same period used for the impregnation experiments (3 weeks). The results for the water-submerged particles, termed 'water', are compared with the raw particles, as shown in Figure 6.5:

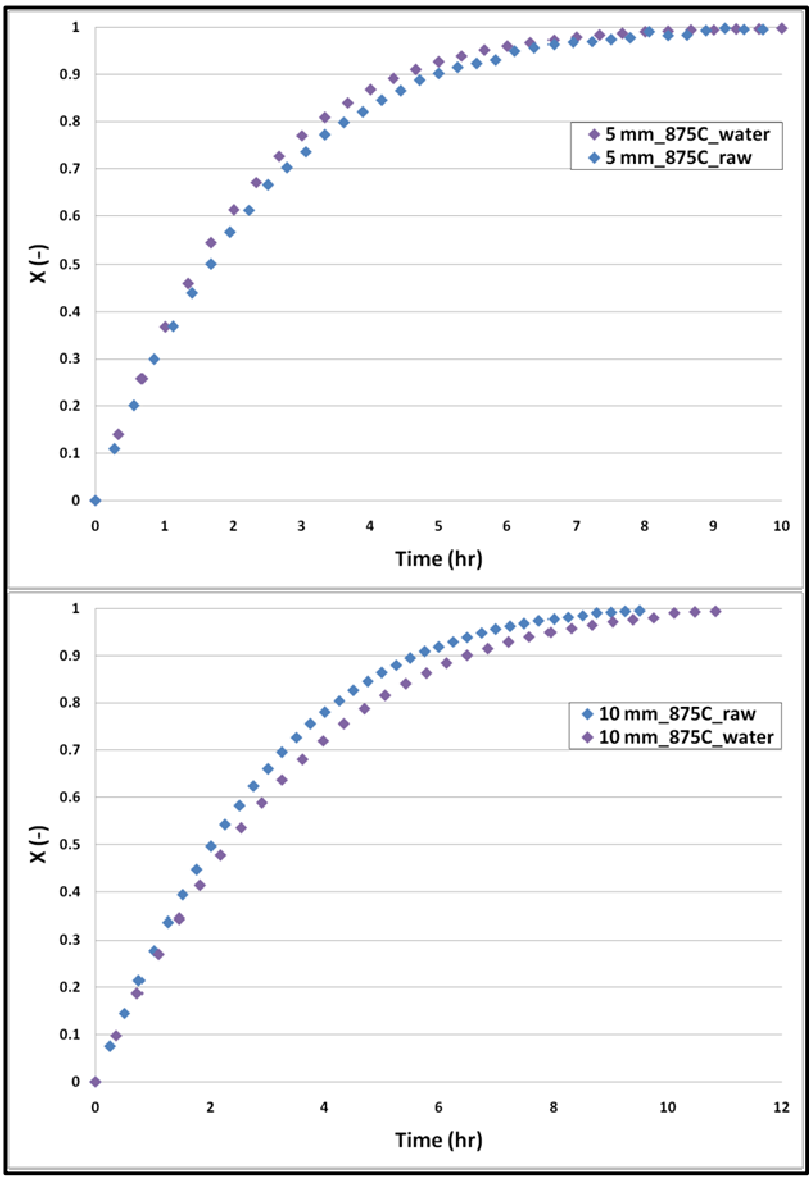

Figure 6.5: Effect of impregnation on reactivity

From the rate profiles presented in Figure 6.5, it can be seen that the reaction rate of the particles submerged in water, closely resembles the results obtained for the raw coal. The reaction rate of the 5 mm submerged particles is slightly higher than the raw coal, while that of the 10 mm submerged particles is lower than the raw coal. This can be attributed to the experimental error of the reactivity experiments. Even though impregnation results in the formation of cracks and alteration of the coal structure, as discussed in Section 5.4.4.1, the

above-mentioned results indicate that this does not influence the reaction rate. Therefore, it can be concluded that any increased reaction rates that may be observed for impregnated particles can be attributed to the catalytic effect.

6.3.3. Factors influencing reactivity

6.3.3.1. Catalytic effect

Conversion data for the raw and catalysed systems were compared in order to determine the catalytic effect. Average conversion data for the 5 mm and 10 mm particles, for both the raw and catalysed samples, are presented in Figure 6.6 and Figure 6.7, respectively:

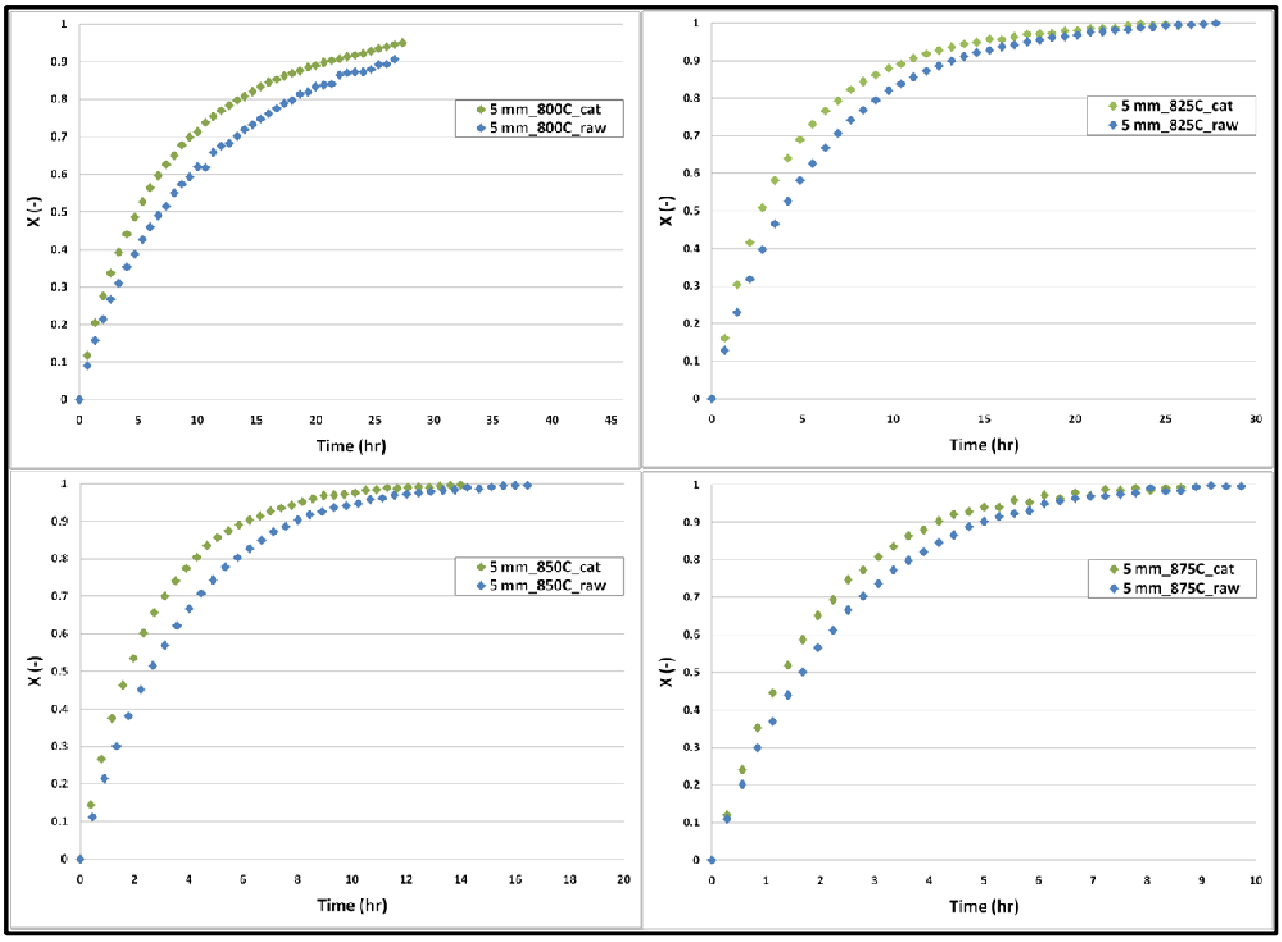

Figure 6.6: Conversion as a function of time, for 5 mm particles

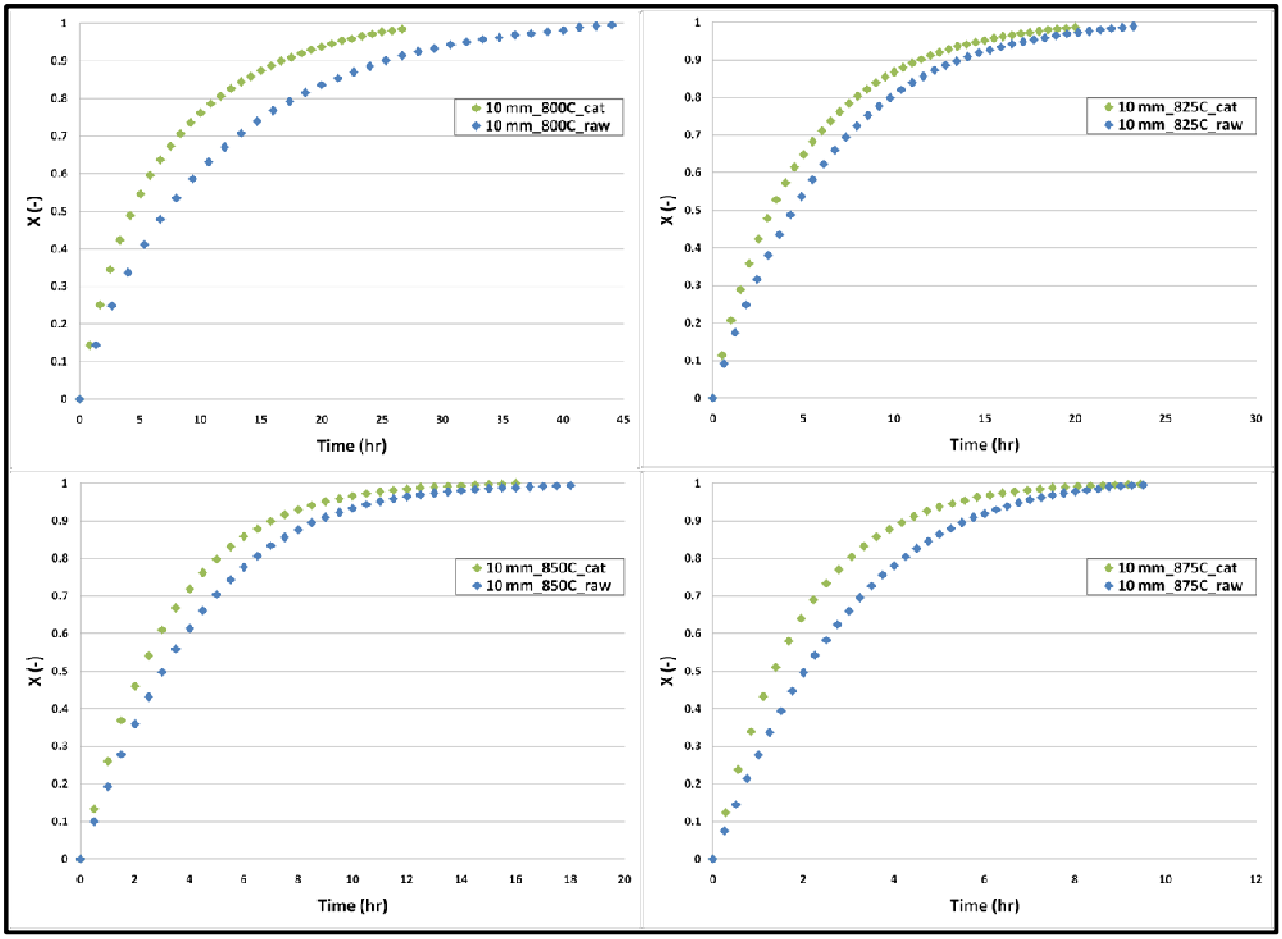

Figure 6.7: Conversion as a function of time, for 10 mm particles

From the conversion rate profiles presented, it can clearly be seen that the addition of K_2CO_3 to the coal samples increases the reaction rate. This is observable for the catalysed samples at all the experimental temperatures. However, the degree by which the reaction rate is enhanced varies. This can be explained by a variation in the catalyst loading for individual coal particles, since the catalytic effect is directly proportional to the catalyst loading. An increase in reaction rate consequently results in a decrease in reaction time to obtain total carbon conversion. From Figure 6.6 and Figure 6.7 it can be seen that catalyst addition decreases the reaction time for all gasification temperatures. The experimental results obtained for the K_2CO_3-catalysed reaction are consistent with results found in literature (Suzuki *et al.*, 1984; Takarada *et al.*, 1986; Yuh and Wolf, 1984; Wang *et al.*, 2009).

6.3.3.2. Temperature influence

In addition to the catalytic effect, experimental temperature also has an influence on the reaction rate of the gasification experiments. The temperature influence on reactivity is illustrated in Figure 6.8.

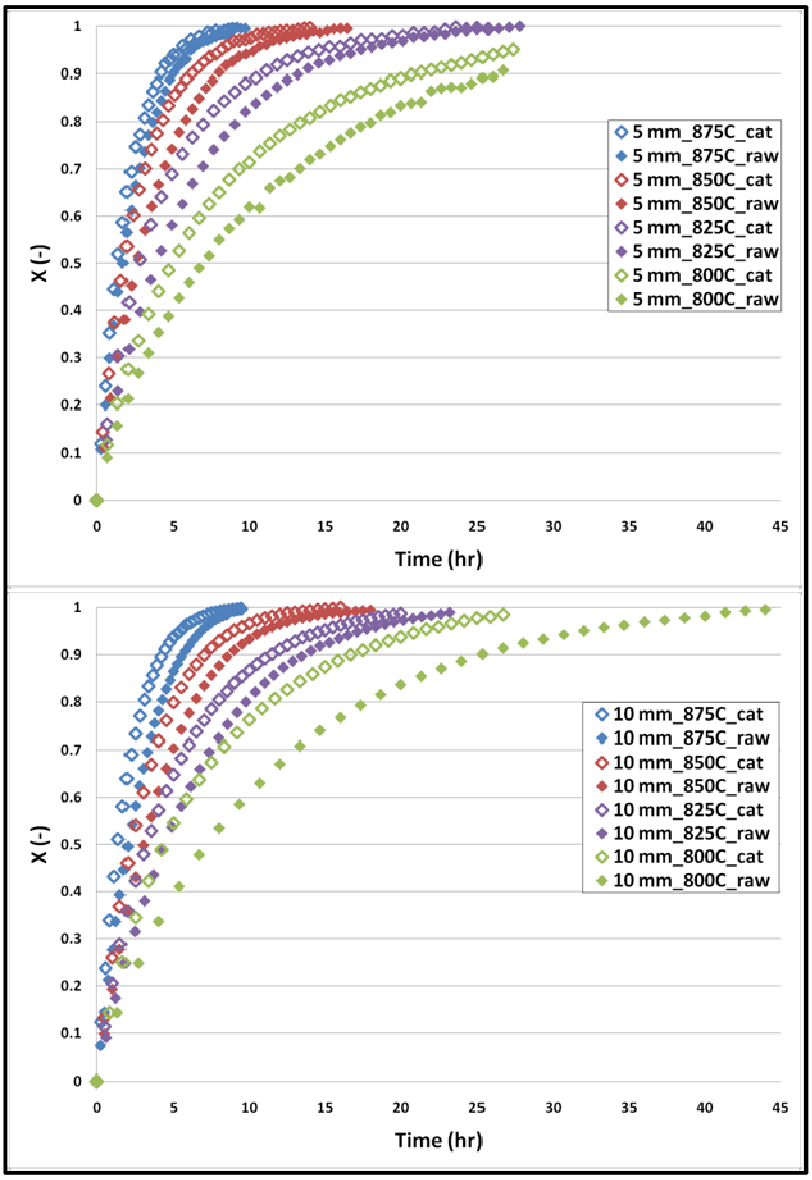

Figure 6.8: Influence of temperature on reactivity

The conversion-time graphs (Figure 6.8) indicate that the reaction rates are sensitive to temperature variations. It can be seen that the reaction rate decreases with a decrease in reaction temperature. The variation in temperature influences the raw, as well as the catalysed reactions. The effect of temperature on steam gasification rates, as seen in this study, has been studied extensively and similar results have been found by other authors

(Schmal *et al.*, 1982; Sharma *et al.*, 2008; Ye *et al.*, 1998). Schmal *et al.* (1982) observed the reaction rate for steam gasification experiments to be very sensitive to temperatures in the range of 800-1000 ℃, and consequently suggested that chemical reaction is the rate-limiting step.

6.3.3.3. Particle size

The influence of particle size on reactivity is illustrated in Figure 6.9:

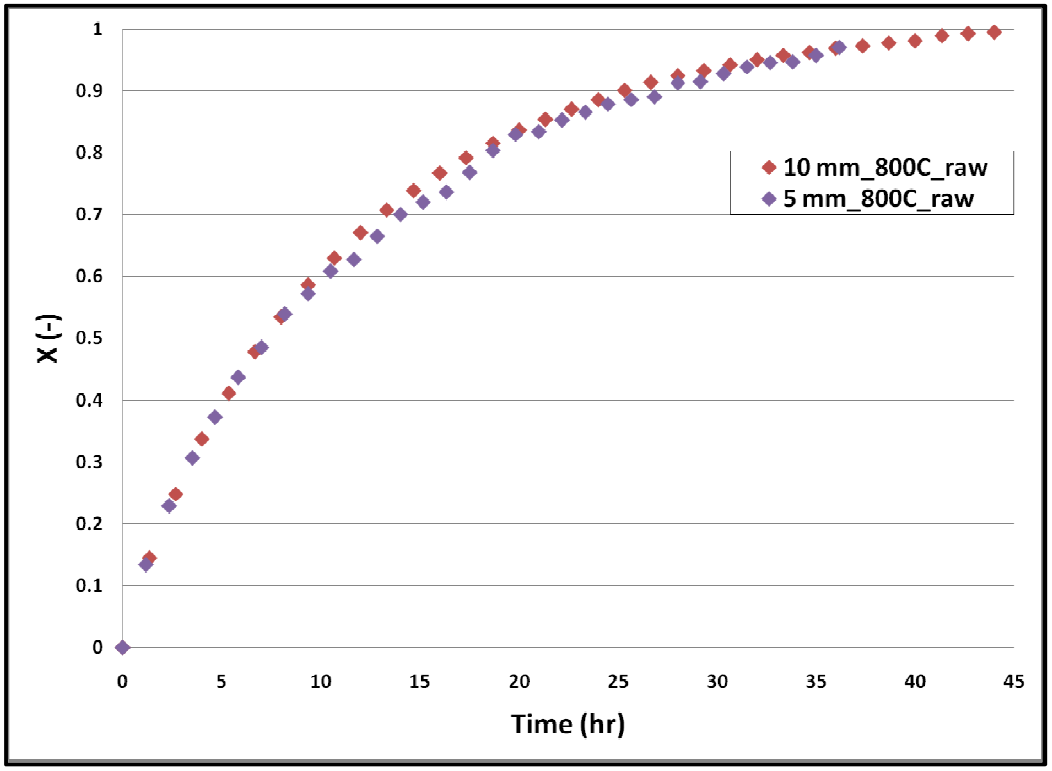

Figure 6.9: Influence of particle size on reactivity at 800 ℃

From the reactivity profiles presented above, it can clearly be seen that the 5 mm and 10 mm particles follow the same conversion trend at 800 ℃. This is also observed at higher experimental temperatures, as presented in Appendix B. The conversion data shows that the gasification time required to reach near complete conversion is similar for the 5 mm and 10 mm particles. From this data it can be concluded that the reaction rate is independent of particle size. This was also observed by other investigators who studied the influence of particle size on gasification rate (Hanson *et al.*, 2002; Ye *et al.*, 1998; Huang and Watkinson, 1996). According to Ye *et al.* (1998), if the reaction rate is independent of particle size, the gasification reactions occur homogeneously throughout the particle and are largely controlled by chemical kinetics. Seeing as though the reaction rates in this study were found

to be particle size independent, this confirms operation in the chemical reaction-controlled regime.

6.3.4. Kinetic evaluation

Numerous models have been proposed to describe the reactions occurring during char gasification. The type of model used depends largely on the purpose of the modelling. Models such as the homogeneous model and un-reacted core model, which do not account for structural changes during gasification, are the most basic kinetic models (Molina and Mondragon, 1998; Zhang *et al*., 2009).

The comparison of reactivities is seen as a simple method to determine the effectiveness of an added catalyst (Takarada *et al*., 1986). For this study, the homogeneous model (HM) is used to determine the reactivities of the raw and catalysed particles, since it is a particle-size-independent model. The heterogeneous gas-solid gasification reaction was reduced to a homogeneous reaction to obtain the homogeneous reaction model. The assumptions made to derive this model are that all sub-particles in the gasification system react uniformly, and that gas-solid reactions occur in all places, both on the exterior and interior of the particles (Molina and Mondragon, 1998; Schmal *et al*., 1982). The reaction rate equation for the homogeneous model is presented by (Molina and Mondragon, 1998):

$$\frac{dX}{dt} = k(1-X) \qquad \text{(Equation 6.2)}$$

where k is the reaction rate constant, and X is the fixed carbon conversion at any given time, t. For the purpose of this investigation, k (reaction rate constant) will be used to indicate the reactivity of the coal. In order to determine the reactivity of the raw and catalysed coal, equation 6.2 is linearised to obtain the following equation:

$$-\ln(1-X) = kt \qquad \text{(Equation 6.3)}$$

The reactivity, k (h^{-1}), is equal to the slope obtained by plotting –ln(1-X) vs. t. Various other investigators have used the homogeneous model to describe steam gasification reactions (Schmal *et al*., 1982; Ishida and Wen, 1968; Shufen and Ruizheng, 1992; Ye *et al*., 1998).

6.3.4.1. Evaluation of reactivity, k (h^{-1})

By using equation 6.3, and plotting –ln(1-X) vs. t, the following graph is obtained for the 10 mm particles at 800 ℃. Similar results were obtained for the 5 mm and 10 mm particles, at all the experimental temperatures.

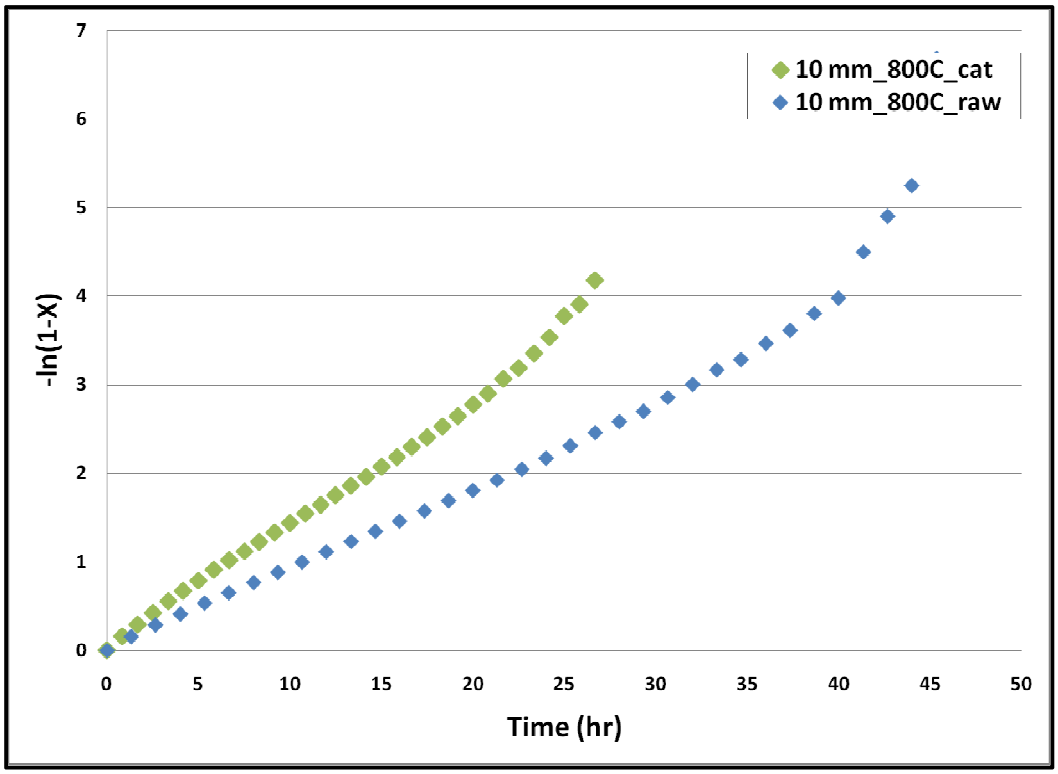

Figure 6.10: Linearised HM plot (-ln(1-X) vs. t)

As seen from Figure 6.10, the trend obtained by plotting the linearised HM is not linear. Therefore, the slope of the data (reactivity) cannot be accurately determined for the entire duration of the reactivity experiments. In order to ensure that the reactivity can be accurately measured, only the linear part of the data presented in Figure 6.10 will be considered. It was found that the data for all the linearised HM plots followed a linear trend up until a fixed carbon conversion of approximately 70 %. Figure 6.11 and Figure 6.12 below shows the plots of –ln(1-X) vs. t, up to 70 % conversion.

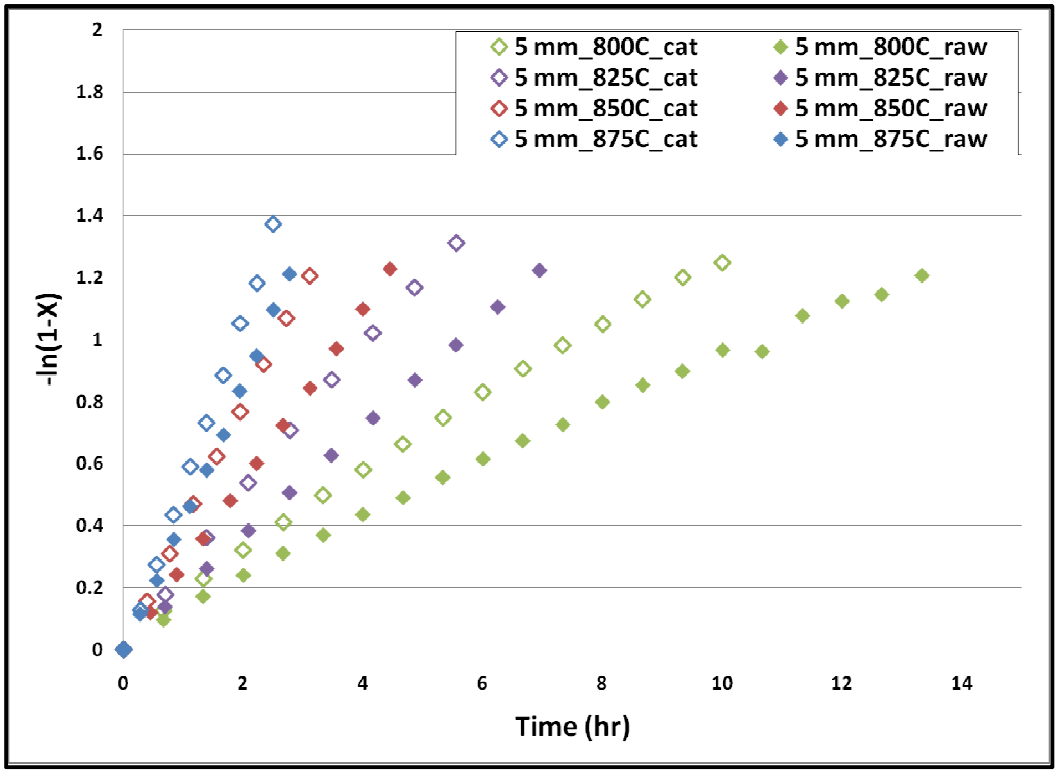

Figure 6.11: Linearised HM plot up to 70 wt.% conversion (5 mm)

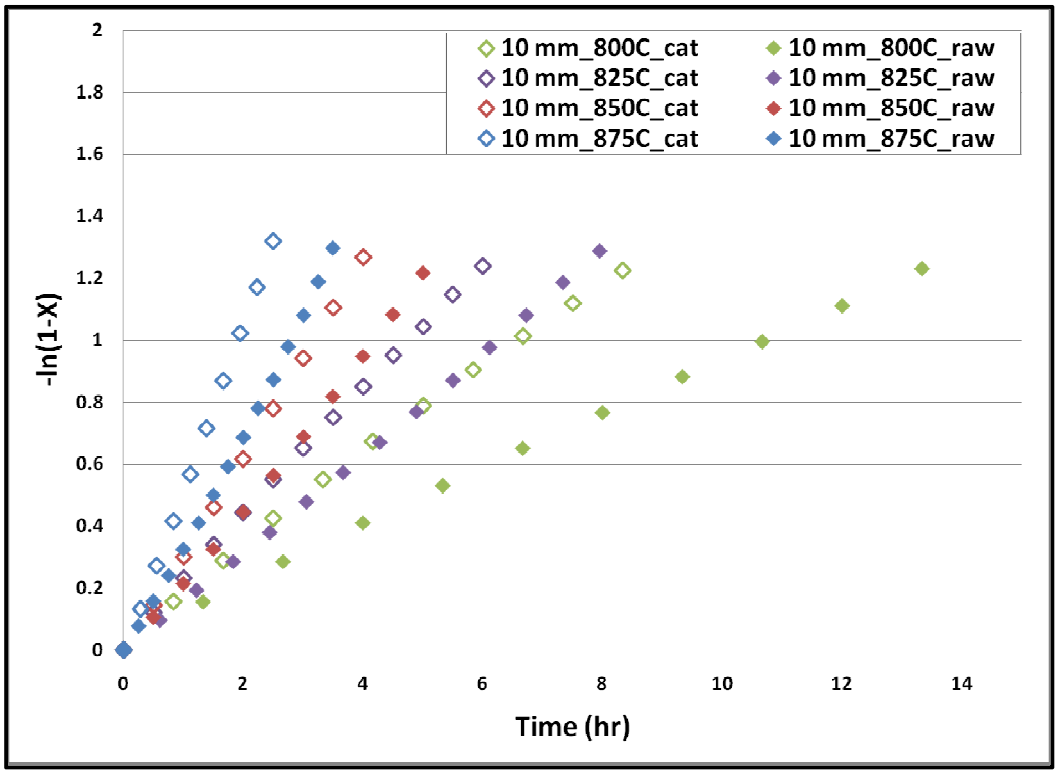

Figure 6.12: Linearised HM plot up to 70 wt.% conversion (10 mm)

As seen from the graphs, the data follow a linear trend up to the specified conversion. These data profiles were used to determine the reactivity of the raw and catalysed coal particles at the various operating temperatures, as presented in Appendix B. The reactivities, k (h^{-1}), determined from data profiles shown in Figure 6.11 and Figure 6.12, are presented in the following table:

Table 6.3: Reactivity values, k (h^{-1})

	5 mm particles		10 mm particles	
Temperature	**Raw (k_{raw})**	**Catalysed (k_{cat})**	**Raw (k_{raw})**	**Catalysed (k_{cat})**
800 °C	0.10 ± 0.01	0.13 ± 0.01	0.09 ± 0.01	0.15 ± 0.01
825 °C	0.18 ± 0.01	0.24 ± 0.02	0.16 ± 0.01	0.21 ± 0.01
850 °C	0.27 ± 0.02	0.39 ± 0.02	0.24 ± 0.02	0.31 ± 0.02
875 °C	0.43 ± 0.03	0.54 ± 0.03	0.36 ± 0.02	0.52 ± 0.03

As seen from the reactivity values presented above, the reactivities of the catalysed coal particles are larger than the reactivities obtained for the raw coal. This is a quantitative confirmation that the addition of K_2CO_3 increases the reaction rate for steam gasification. An average increase in reactivity of 1.4 times is obtained with the addition of the catalyst, for both the 5 mm and 10 mm particles. Thus, there is no significant difference in reactivity enhancement as a result of catalyst loading variation. It can therefore be said that the different catalyst loadings obtained for the 5 mm (0.83 wt.% K) and 10 mm (0.76 wt.% K) particles did not affect the degree by which the reactivity is increased, since these loadings are relatively low. The reactivity values also indicate that the reactivity of both the raw and catalysed coal increases with increasing temperature. This was also observed by other investigators (Schmal *et al.*, 1982; Guzman and Wolf, 1982; Lee and Kim, 1995).

For the purpose of this study, the catalytic effectiveness is defined as the ratio of the reactivity of the catalysed coal to the reactivity of the raw coal (k_{cat}/k_{raw}). The catalytic effectiveness for the different particle sizes, at the various experimental temperatures, is presented in Table 6.4:

Table 6.4: Catalytic effectiveness

Temperature	5 mm (k_{cat}/k_{raw})	10 mm (k_{cat}/k_{raw})
800 °C	1.4	1.6
825 °C	1.4	1.3
850 °C	1.4	1.3
875 °C	1.3	1.5

Results show no significant trend for the catalytic effectiveness obtained for the 5 mm and 10 mm experiments. Hippo and Tandon (1996) found that the catalytic effect decreased with increasing temperature, as a result of catalyst deactivation. Deactivation of the catalyst can occur as a result of agglomeration, catalyst poisoning, and/or volatilisation of the catalyst, which can become more severe at higher temperatures (Hippo and Tandon, 1996; Nishiyama, 1991). The results presented in Table 6.4 do not indicate a definite decrease in catalytic effectiveness with increasing gasification temperature, and therefore no concrete conclusion can be made regarding catalyst deactivation.

6.3.4.2. Evaluation of activation energy, E_a (kJ/mol)

The Arrhenius expression, as presented in equation 6.4, was used to evaluate the activation energies of the raw and catalysed systems:

$$k = A\exp\left(\frac{-E_a}{RT}\right) \qquad \text{(Equation 6.4)}$$

$$\ln k = \ln A + \left(\frac{-E_a}{R}\right)\left(\frac{1}{T}\right) \qquad \text{(Equation 6.5)}$$

The linearised form of the Arrhenius equation is represented by equation 6.5, and is used to obtain Arrhenius plots. The relationship between the reactivity, k, and the reciprocal of the experimental temperature is given by the Arrhenius plot. Figure 6.13 presents the combined Arrhenius plot for the 5 mm and 10 mm particles. The reactivity results of the 5 mm and 10 mm particles are combined on an Arrhenius plot, since the reaction rates are independent of particle size.

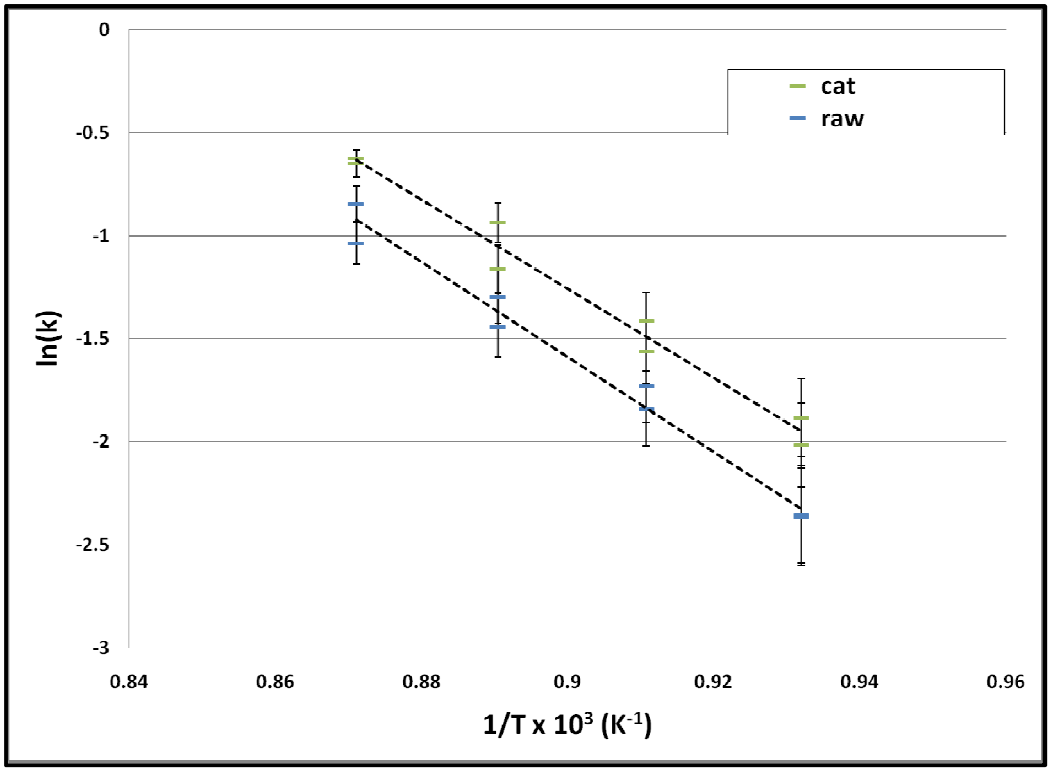

Figure 6.13: Combined Arrhenius plot for 5 mm and 10 mm particles

From the figure presented above, it can clearly be seen that a linear relation exists between the reactivity and the reciprocal of the reaction temperature, which indicates that the steam gasification reactions are accurately described by the Arrhenius law. The Arrhenius plots for the catalysed reactions are linear, which indicate a continuous increase in reaction rate as the gasification temperature increases. By conducting experiments at temperatures below the melting point of the catalyst, it prevents the catalyst from melting and spreading over the particle surface, which causes an irregular catalytic effect (McKee and Chatterji, 1978; Freriks *et al*., 1981; Veraa and Bell, 1987). The activation energies determined from the Arrhenius plots are presented in Table 6.5, along with activation energies obtained by other investigators, for steam gasification reactions.

Table 6.5: Activation energies, E_a (kJ/mol)

	Raw	Catalysed	Coal	Temperatures
This investigation	191 ± 11	179 ± 9	WashedHighveld coal	800-875 °C
Everson *et al.* (2006)	143 ± 14	-	Highveld coal	750-950 °C
Lu and Do (1992)	170	-	Char	800-950 °C
Wu *et al.* (2006)	127-197	-	Yanzhou coal	900-1200 °C
Lee and Kim (1995)	211	185	Sub-bituminous	700-850 °C
Veraa and Bell (1978)	206	164-188	Wyoming coal	700-900 °C

The activation energies obtained for the raw coal in this investigation correlate well with published data, as seen in Table 6.5. From the results presented above, a decrease in activation energy is observed with the addition of a catalyst. The activation energy obtained by Everson and co-workers, for Highveld coal, is lower when compared to the value obtained for this investigation (raw coal). This can be attributed to the relatively high ash content of the coal used by Everson *et al.* (2006). The catalytically active compounds in the ash can increase the coal reactivity and consequently reduce the activation energy (Hattingh, 2009). In comparison with the values obtained by Lee and Kim (1995) and Veraa and Bell (1978), the reduction in activation energy for this study was not as significant. This can be attributed to the different catalyst loadings, since the catalytic effect and consequently the activation energy, is dependent on the catalyst loading. Lee and Kim (1995) selected a loading of 6 wt.% K, while Veraa and Bell (1978) used 5 wt.% and 10 wt.% loadings (K). It can, however, be concluded that a slight decrease in activation energy is observed for relatively low catalyst loadings ranging from 0.76 wt.% to 0.83 wt.% K.

6.3.5. Surface effect of catalyst addition

Raw and impregnated coal samples were de-volatilised at 875 °C, in order to study the catalytic influence on the char structure. Figure 6.14 and Figure 6.15 illustrate the raw and impregnated char samples of 5 mm and 10 mm particles, respectively. The images were taken with a light microscope, at a scale of 2000 µm.

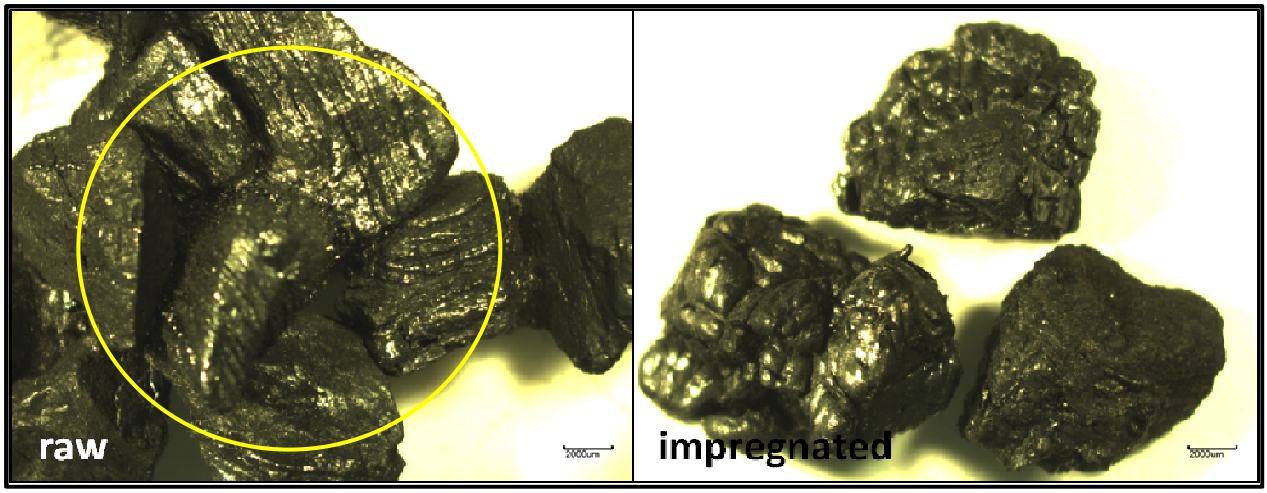

Figure 6.14: Char samples of raw and impregnated 5 mm particles

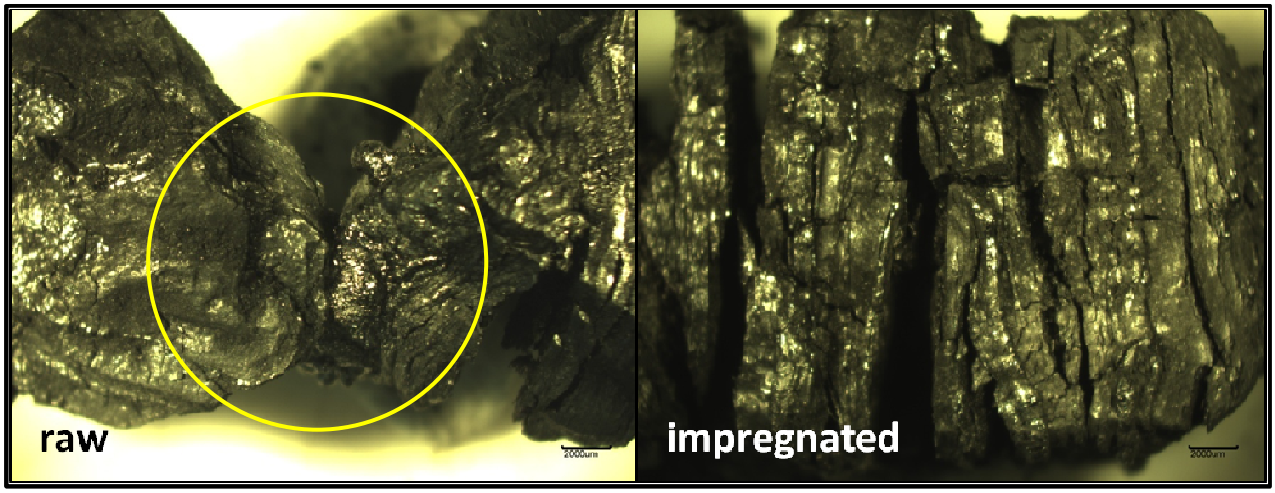

Figure 6.15: Char samples of raw and impregnated 10 mm particles

From the images presented above, it can clearly be seen that de-volatilisation of the raw coal particles resulted in the agglomeration of the char. The highlighted areas in the images indicate where the raw char samples are fused together. The opposite is observed for the impregnated char samples. The images of the impregnated char samples show that the catalyst-containing particles did not agglomerate during devolatilisation. From these observations it can be concluded that the presence of a catalyst reduces the tendency for the coal to agglomerate. Similar results were observed in other studies (Gallagher Jr. and Euker Jr., 1979; Suzuki *et al.*, 1984; McCormick and Jha, 1995).

SEM images of the 5 mm char samples at different scales are presented in Figure 6.16 and Figure 6.17.

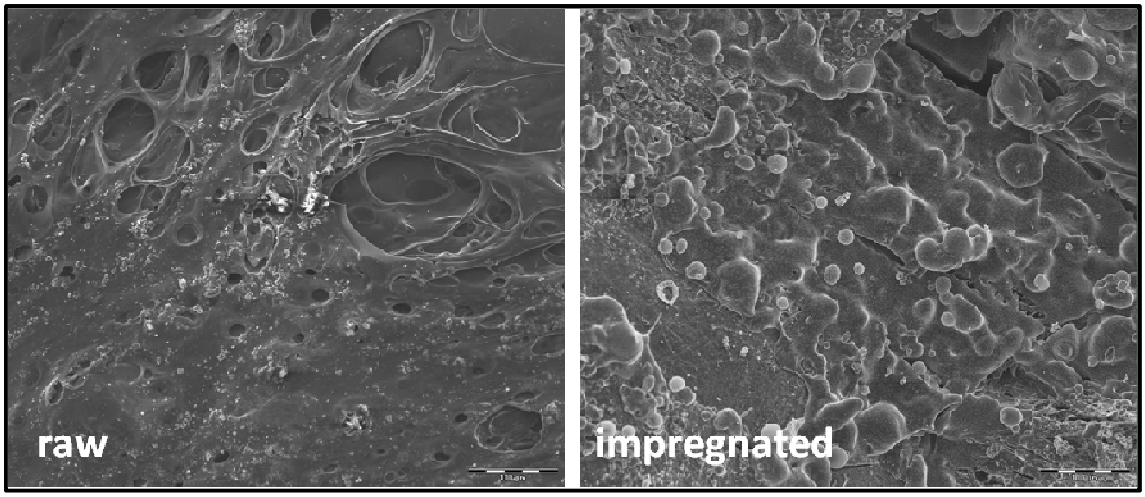

Figure 6.16: SEM scans of 5 mm char samples (100 µm)

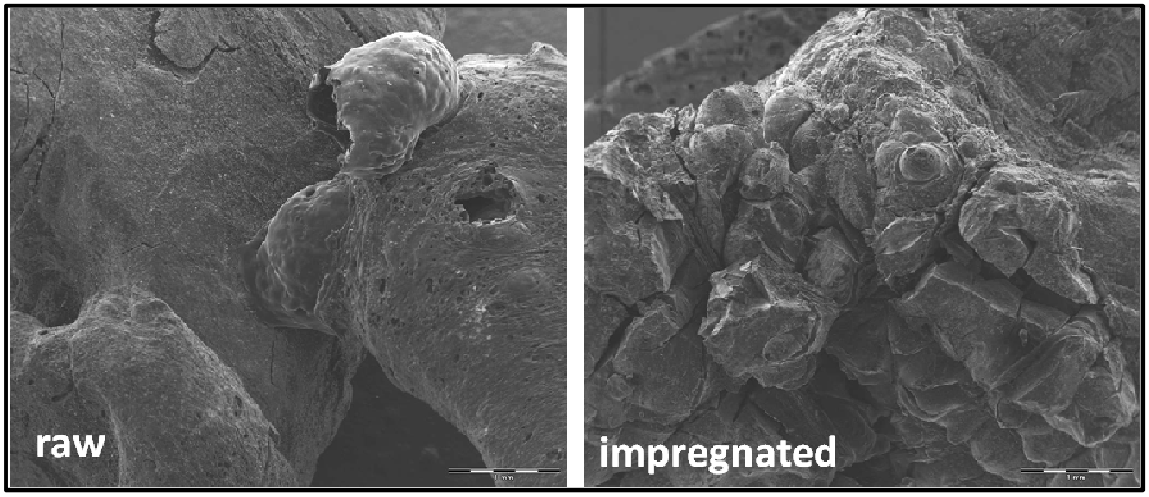

Figure 6.17: SEM scans of 5 mm char samples (1 mm)

The SEM images presented above clearly show the effect of catalyst addition on the surface structure during devolatilisation. The raw char in Figure 6.16 has a relatively smooth, molten surface, while the surface of the impregnated char is much more irregular, with nodules distributed across the surface. Figure 6.17 (raw) shows two raw char particles fused together during devolatilisation, with the charred particles having a relatively smooth surface. In contrast, the impregnated char samples have a jagged, porous surface structure. Similar results were obtained by Timpe *et al.* (1987). According to the authors, increased reactivity due to catalyst addition is caused by a change in the mechanism of the chemical reaction, as well as physical change. It was found that the addition of a catalyst increased the surface area of the char, and consequently resulted in an increase in available active sites (Timpe *et al.*, 1987).

6.4. Summary

The impregnation method discussed in Section 5.3.3.1 was used to impregnate 5 mm and 10 mm coal particles with K_2CO_3. Steam gasification experiments were carried out to determine the effect of catalyst addition on the reaction rate. Steam reactivity experiments were conducted at temperatures ranging from 800 °C to 875 °C. The experimental results presented in Section 6.3 are subsequently summarised:

- Conversion-time profiles indicated that the addition of K_2CO_3 to the coal particles increased the steam gasification reaction rate. This was quantitatively confirmed by the reactivities determined from the linearised HM plots.
- It was found that an increase in experimental temperature resulted in an increase in reaction rate, for both the raw and catalysed systems, and that the reaction rate was independent of particle size.
- A slight decrease in activation energy was observed with the addition of K_2CO_3.
- The addition of potassium carbonate appeared to reduce agglomeration of the chars.